

THERMOLUMINESCENCE DOSIMETRY OF A THERMAL NEUTRON FIELD AND COMPARISON WITH MONTE CARLO CALCULATIONS

A. C. Fernandes^{1,2,*}, J. P. Santos¹, A. Kling^{1,2}, J. G. Marques^{1,2}, I. C. Gonçalves¹, A. Ferro Carvalho¹, L. Santos¹, J. Cardoso¹ and M. Osvey³

¹Instituto Tecnológico e Nuclear, Estrada Nacional 10, P-2686-953 Sacavém, Portugal

²Centro de Física Nuclear da Universidade de Lisboa, Av. Prof. Gama Pinto, no. 2, P-1649-003 Lisboa, Portugal

³Institute of Isotope and Surface Chemistry, Budapest P.O. Box 77, H-1525, Hungary

The characteristics of thermoluminescence dosimeters (TLDs) regarding the determination of photon and neutron absorbed doses were investigated in a thermal neutron beam. Harshaw TLD-100 (LiF:Mg,Ti) and TLD-700 (⁷LiF:Mg,Ti) were compared with similar materials from Solid Dosimetric Detector and Method Laboratory (People's Republic of China). Harshaw TLD-700H (⁷LiF:Mg,Cu,P) and aluminium oxide (Al₂O₃:Mg,Y) from Hungary were also considered for photon dose measurement. The neutron sensitivity of the investigated materials was measured and found to be consistent with values reported by other authors. A comparison was made between the TL dose measurements and results obtained via conventional methods. An agreement within 20% was obtained, which demonstrates the ability of TLD for measuring neutron and photon doses in a mixed field, using careful calibration procedures and determining the neutron sensitivity for the usage conditions.

Radiation fields at nuclear reactors are usually comprised of different kinds of particles, whose contributions to absorbed doses must be discriminated. Thermoluminescence dosimeters (TLDs) have been used for measuring the photon and thermal neutron doses in such mixed radiation fields⁽¹⁾. Paired detectors having different thermal neutron sensitivities—ideally with one of them insensitive to neutrons—are applied.

The application of LiF:Mg,Ti TLDs (e.g. TLD-100 and TLD-700) has evidenced difficulties arising from a small ⁶Li content in the photon dosimeters⁽²⁾, a sensitivity loss in the neutron sensitive materials⁽³⁾ and a supralinear response at the dose levels commonly encountered⁽¹⁾. The properties of LiF:Mg,Cu,P have been investigated intensively and it was demonstrated that this material is one of the least sensitive to neutrons⁽⁴⁾, but its application should be restricted to low dose levels, otherwise a sensitivity loss caused by radiation damage occurs⁽⁵⁾. Ceramic aluminium oxide Al₂O₃:Mg,Y TL detectors were explicitly developed for high dose measurement purposes and are of special interest for photon measurements in nuclear reactors, since their thermal neutron sensitivity is comparable with the photon dosimeters mentioned previously⁽⁶⁾.

The accuracy of TL measurements is frequently assessed via a comparison between measured and calculated neutron and photon doses. There is generally a good agreement between the measured and calculated dose profiles, but this does not necessarily

apply to the absolute dose values. These differences are frequently attributed to the high uncertainty in the detector sensitivity to thermal neutrons⁽²⁾. The strong discrepancy among values reported in the literature⁽¹⁾ suggests the need to determine the neutron sensitivity for the detectors and evaluation conditions used.

In this work, the mixed radiation field at a thermal neutron beam of the Portuguese Research Reactor (RPI) has been characterised using conventional reactor dosimetry methods (Monte Carlo simulation and activation foil measurements) and various TLDs (LiF:Mg,Ti, LiF:Mg,Cu,P and Al₂O₃:Mg,Y). Once thoroughly characterised, this thermal neutron field was applied to the study of important dosimetric characteristics of the referred TLDs, namely their thermal neutron sensitivity. A comparison of results is performed in order to make a comprehensive assessment of the TLDs ability for mixed-field dosimetry at a nuclear reactor.

MATERIALS AND METHODS

The mixed radiation field at the vertical access of the thermal column of RPI was simulated with the MCNP code⁽⁷⁾ using a detailed model which includes the reactor core⁽⁸⁾. The calculated neutron spectrum was adjusted further via the multiple-foil activation method. Aluminium-diluted detectors of Au, Mn, In, Dy and pure Sc (bare and covered with 1 mm of cadmium) were applied for this purpose. Spectrum unfolding was performed using the LSLM-2 code⁽⁹⁾. The thermal and epithermal self-shielding effect for the Sc foil was estimated^(10,11). Gold foils

*Corresponding author: anafer@itn.mces.pt

at a fixed position were used to monitor the neutron fluence in each irradiation. Detector activities were measured with a HP(Ge) spectrometry system.

For determining the calculated neutron and photon doses, tabled point-wise kerma factors⁽¹²⁾ and energy absorption coefficients⁽¹³⁾ were converted into group values using the FLXPRO code included in the LSLM package and considering the calculated neutron and photon spectra as weighting spectra. The uncertainties (reported at the 1-sigma level) in the calculated doses included those from calculated spectra, flux-to-dose conversion factors and normalisation factors.

Thermoluminescence measurements of neutron and photon doses at the irradiation facility were performed using TLD-100 (^{nat}LiF:Mg,Ti chips, $3.1 \times 3.1 \times 0.9$ mm³; Harshaw) and TLD-700H (⁷LiF:Mg,Cu,P chips, $3.2 \times 3.2 \times 0.4$ mm³; Harshaw), respectively. In addition, TLD-700 (⁷LiF:Mg,Ti; Harshaw) and Al₂O₃:Mg,Y (D-3 disks, 8×1 mm²; Institute of Isotope and Surface Chemistry, IKI, Hungary) were applied to determine the photon doses. Finally, TLD-100 and TLD-700 were compared with the similar materials GR-100 and GR-107 ($4 \times 4 \times 0.8$ mm³; Solid Dosimetric Detector and Methods Laboratory, SDDML, People's Republic of China), respectively.

Individual calibrations were performed for all detectors. For each material, a control group of five detectors was irradiated by a ⁶⁰Co source of the Metrology Laboratory of Ionising Radiations and Radioactivity. The air kerma for the control dosimeters was 100 mGy (LiF) and 1 Gy (Al₂O₃).

For irradiation, the detectors were encapsulated in 5 mm thick black polymethylmethacrylate (PMMA). Exposure to light was avoided by storing the dosimeters under black polyethylene foil.

The dosimeters were annealed (LiF:Mg,Ti: 400°C, 1 h + 100°C, 2 h + fast cooling; D-3: 600°C, 1 h + slow cooling) between irradiations and evaluated 24 h after the irradiation with a Harshaw 3500 reader (at 5 °C s⁻¹). TLD-700H detectors were regenerated directly with the TL reader and background subtraction was performed by reading the detectors twice (up to 250 °C). The low and high temperature peaks of LiF:Mg,Ti (137–255°C and 255–370°C, respectively) were integrated separately.

EXPERIMENTS AND RESULTS

Characterisation of the radiation field

Figure 1 shows a sketch of the irradiation facility, also used as the MCNP model for calculating the mixed radiation field. Measurements with bare and Cd-covered gold foils evidenced a homogeneous neutron field along lines parallel to the core, although decreasing in the perpendicular direction. The bare and covered activation foils used for adjusting the calculated neutron spectrum were irradiated in a fixed position at a reactor power of 1 MW, during 4 and 10 h, respectively. Table 1 presents the measured foil responses and the calculated responses, both in the calculated and adjusted neutron spectra. These spectra and the region corresponding to 90% of detector response (i.e. the 5 and 95% limits) are shown in Figure 2. The adjusted thermal and epithermal neutron fluence rates at the irradiation facility are $4 \times 10^7 \pm 4\%$ and 2×10^5 cm⁻² s⁻¹ $\pm 6\%$, respectively. The complete spectrum-averaged neutron dose rate in air is 1.2 Gy h⁻¹ $\pm 12\%$. Thermal neutrons (energy <0.5 eV) are responsible for 98% of the total neutron dose.

The Monte Carlo model overestimates the relative thermal neutron component by ~40%. This effect

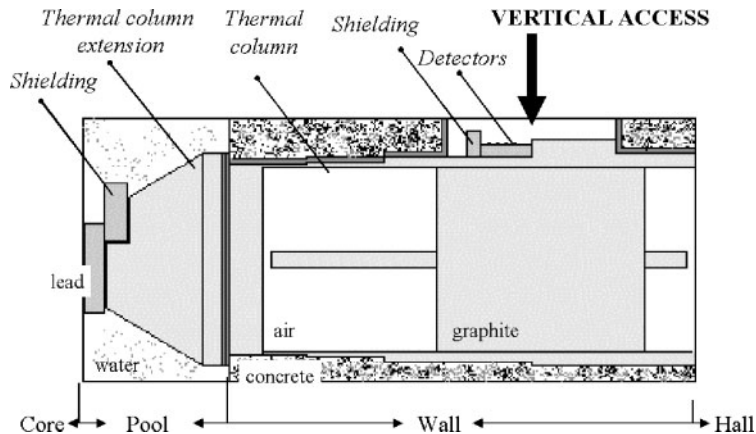


Figure 1. MCNP model of the vertical access of the thermal column of RPI.

Table 1. Measured foil responses and comparison with calculated (C) and adjusted (A) responses.

Reaction	M (10^{-15} s^{-1})	C/M	A/M	90% Response
$^{45}\text{Sc}(n,\gamma)^{46}\text{Sc}$	$0.971 \pm 3.5\%$	1.09	1.05	5.4 meV–0.22 eV
$^{45}\text{Sc}(n,\gamma)^{46}\text{Sc}$ (Cd)	$0.00390 \pm 4.1\%$	0.62	0.98	0.14–74 eV
$^{55}\text{Mn}(n,\gamma)^{56}\text{Mn}$	$0.515 \pm 3.2\%$	1.03	0.99	5.4 meV–0.22 eV
$^{115}\text{In}(n,\gamma)^{116}\text{In}$	$9.44 \pm 3.5\%$	1.13	1.03	5.9 meV–1.1 eV
$^{115}\text{In}(n,\gamma)^{116}\text{In}$ (Cd)	$0.673 \pm 9.9\%$	0.68	1.03	0.78–1.9 eV
$^{164}\text{Dy}(n,\gamma)^{165}\text{Dy}$	$96.1 \pm 12.0\%$	1.01	1.00	5.5 meV–0.19 eV
$^{164}\text{Dy}(n,\gamma)^{165}\text{Dy}$ (Cd)	$0.147 \pm 13.6\%$	0.62	1.01	0.12 meV–4.3 eV
$^{197}\text{Au}(n,\gamma)^{198}\text{Au}^a$	$4.10 \pm 2.4\%$	1.00	1.02	5.9 meV–2.9 eV
$^{197}\text{Au}(n,\gamma)^{198}\text{Au}$ (Cd)	$0.279 \pm 3.7\%$	0.67	1.02	1.9–10 eV

^aNormalisation reaction.

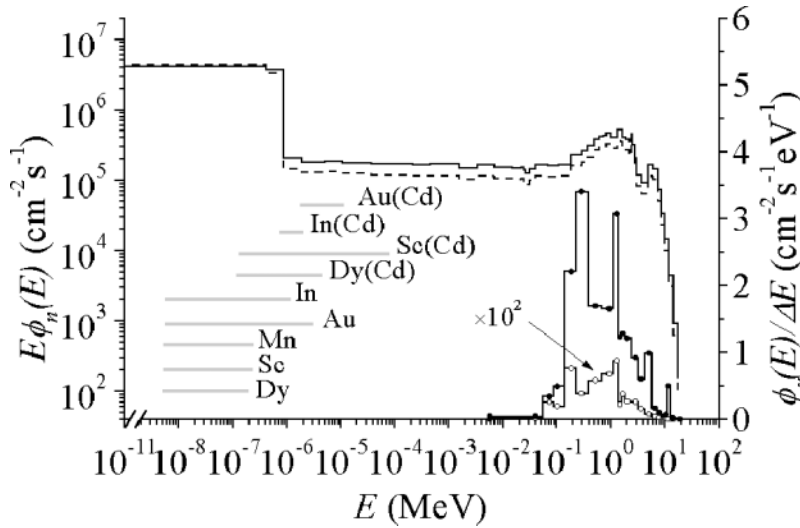


Figure 2. Spectra of neutron fluence rate per unit lethargy (dashed lines, calculated and solid lines, adjusted), calculated spectra of photon fluence rate per unit energy (solid lines with open circles, reactor background and solid lines with closed circles, total) and 90% response region of the activation reactions considered for neutron spectrum unfolding (thick solid lines).

may be caused by impurities in the lead shielding (Sb contamination), graphite and pool wall lining (unknown amount of steel-nobles). Correspondingly, the calculated responses of the covered detectors are $\sim 40\%$ lower than the measured ones, since the normalisation reaction responds mostly to the thermal region. However, the discrepancies are consistent and thus a good agreement (within 5%) between the adjusted and measured foil responses was obtained. The largest discrepancies were observed for the Sc foil that suffers from the highest self-shielding effect.

The MCNP-calculated photon spectrum (Figure 2) discriminates the components due to (i) reactor background (fission and capture reactions in the pool) and (ii) neutron capture within the thermal

column. The calculated photon spectrum exhibits peaks originating from neutron capture reactions in the PMMA support (2.2 MeV) and in the lead shielding (600 keV and 7.4 MeV), and also the characteristic X rays of lead (between 70 and 90 keV). According to the calculations, the reactor background has a negligible contribution ($\sim 0.2\%$) to the total photon dose, which may therefore be normalised to the adjusted neutron fluence. The total photon dose rate in air is $114 \text{ mGy h}^{-1} \pm 8\%$.

TL measurements

The TLDs were placed along lines perpendicular to the core, so that on the average every material received the same photon and neutron dose. The

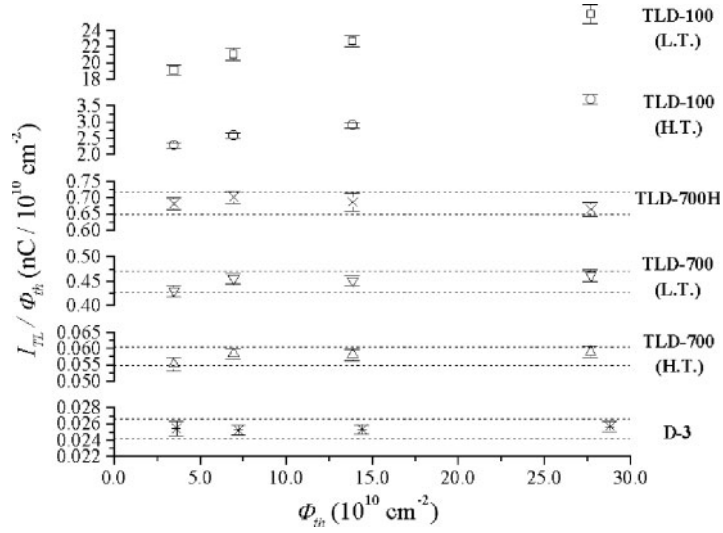


Figure 3. Ratio of TL response to neutron fluence of selected TL materials irradiated at the vertical access of the thermal column, as a function of the thermal neutron fluence. The 5% limits are indicated by the dashed lines (L.T., low temperature peaks and H.T., high temperature peaks).

Table 2. Thermal neutron sensitivity of the investigated TLDs (mGy $^{60}\text{Co}/10^{10} \text{ n}_{\text{th}} \text{ cm}^{-2}$).

	TLD-100	TLD-700	GR-100	GR-107	TLD-700H	D-3
Low temperature	1110	20	630	7	5	4
High temperature	6100	190	4560	20	—	—
Literature ^(1,4,6)	650–5350	2–25	—	0.8–10	0.08–8.3	4

linearity of TL response in the mixed-field was investigated by irradiating at constant dose rate during different irradiation times. Figure 3 illustrates the supralinear behaviour of both low and high temperature peaks of LiF:Mg,Ti. For TLD-100, the sensitivity increase between irradiations with 4×10^{10} and $3 \times 10^{11} \text{ cm}^{-2}$ neutron fluence was 40% (low temperature peaks) and 60% (high temperature peaks), while for GR-100 the increase was 30% (low temperature peaks) and 40% (high temperature peaks). The detectors with low neutron sensitivity exhibited a linear response within 5%.

The neutron sensitivity of the TL materials was calculated based on the ratio of the TL yield in the mixed-field (1 h at 1 MW) and for a reference photon dose (1 Gy of ^{60}Co). The neutron sensitivity was calculated relative to the one of D-3 and finally normalised to the value reported for this material⁽⁶⁾. Table 2 presents the neutron sensitivity of the TL materials used, expressed in units of gamma sensitivity. The values obtained by other authors^(1,4,6) are included and show that the measured neutron sensitivities are consistent with reported values. The neutron sensitivity of the low temperature peaks of

Harshaw LiF is 2–3 times higher than for similar materials from SDDML. This shows that GR-107 is a better photon discriminator than TLD-700. However, for low dose neutron measurements TLD-100 will have an advantage over GR-100. Aluminium oxide and TLD-700H have similar neutron sensitivities.

The neutron and photon doses in the thermal neutron field were measured at similar irradiation conditions as used for determining the neutron sensitivity. The measured neutron dose was derived from the TL signal, considering a kerma factor of $5.95 \times 10^{-12} \text{ Gy cm}^2$ for converting thermal neutron fluence into neutron dose. The measured photon and neutron dose rates in air were $100 \text{ mGy h}^{-1} \pm 12\%$ and $1.4 \text{ Gy h}^{-1} \pm 20\%$, respectively. These results agree with those calculated by the Monte Carlo model within 20%.

CONCLUSIONS

The mixed radiation field at the vertical access of the thermal column of RPI was simulated using the MCNP code. The agreement between measured and

calculated neutron doses demonstrates both, the ability of the MCNP model for simulating the neutron component of the radiation field, and the consistency of determined TL neutron sensitivities. Furthermore, the good agreement obtained in the case of the photon component shows that an MCNP model can predict well the photon field in a reactor-based irradiation facility, if the dose contributions from the fission and decay photons are negligible. The results corroborate the advantage of calibrating TL detectors at dose levels and evaluating conditions similar to those expected in the experiment. In spite of the sensitivity loss exhibited by materials with high neutron sensitivity, thermoluminescence dosimetry can be regarded as a suitable method for mixed-field dosimetry at a nuclear reactor, once careful calibration procedures are followed.

ACKNOWLEDGEMENTS

The authors wish to thank the RPI operation group for providing the irradiations in the thermal column.

REFERENCES

1. Horowitz, Y. S. *Neutron dosimetry*. In: Thermoluminescence and Thermoluminescent Dosimetry. Horowitz, Y. S., Ed., Vol. II (Boca Raton, FL: CRC Press) pp. 90–114 (1984).
2. Aschan, C., Toivonen, M., Seppälä, T. and Auterinen, I. *Epithermal neutron beam dosimetry with thermoluminescence dosimeters for Boron Neutron Capture Therapy*. Radiat. Prot. Dosim. **81**, 47–55 (1999).
3. Fernandes, A. C., Gonçalves, I. C., Ferro Carvalho, A., Santos, J., Cardoso, J., Santos, L. and Osvay, M. *Reproducibility of TL measurements in a mixed field of thermal neutrons and photons*. Radiat. Prot. Dosim. **101**, 481–484 (2002).
4. Wang, S. S., Cai, G. G., Zhou, K. Q. and Zhou, R. X. *Thermoluminescence response of $^6\text{LiF:Mg,Cu,P}$ and $^7\text{LiF:Mg,Cu,P}$ TL chips in neutron and gamma-ray mixed radiation fields*. Radiat. Prot. Dosim. **33**, 247–250 (1990).
5. Muniz, J. L. and Delgado, A. *A study of LiF GR-200 for radiotherapy mailed dosimetry*. Phys. Med. Biol. **42**, 2569–2576 (1997).
6. Osvay, M. *Measurements on shielding experiments using $\text{Al}_2\text{O}_3\text{:Mg,Y}$ TL detectors*. Radiat. Prot. Dosim. **66**, 217–219 (1996).
7. Briesmeister, J., Ed. *MCNP—a general Monte Carlo N-Particle transport code system, version 4C*. LA-13709-M, (Los Alamos, NM, Los Alamos National Laboratory) (2000).
8. Fernandes, A. C., Gonçalves, I. C., Barradas, N. P. and Ramalho, A. J. *Monte Carlo modeling of the Portuguese Research Reactor and comparison with experimental measurements*. Nucl. Technol. **143**, 358–363 (2003).
9. Stallmann, F. W. *LSL-M2: a computer program for least-squares logarithmic adjustment of neutron spectra*. ORNL/TM-9933 (Oak Ridge, TN, Oak Ridge National Laboratory) (1986).
10. Fleming, R. F. *Neutron self-shielding factor for simple geometries*. Appl. Radiat. Isot. **33**, 1263–1268 (1982).
11. Martinho, E., Gonçalves, I. F. and Salgado, J. *Universal curve of epithermal neutron resonance self-shielding factors in foils, wires and spheres*. Appl. Radiat. Isot. **58**, 371–375 (2003).
12. Chadwick, M. B. and 12 others. *A consistent set of neutron kerma coefficients from thermal to 150 MeV for biologically important materials*. Med. Phys. **26**, 974–991 (1999).
13. Hubbell, J. H. and Seltzer, S. M. *Tables of X-ray mass attenuation coefficients and mass energy-absorption coefficients (version 1.03)*. NIST IR 5632 (Gaithersburg, MD: National Institute of Standards and Technology) (1995).